Tashiro *et al.*
Progress in Earth and Planetary Science (2024) 11:17
https://doi.org/10.1186/s40645-024-00619-w

Progress in Earth and Planetary Science

RESEARCH ARTICLE

Open Access

Impact of permafrost degradation on the extreme increase of dissolved iron concentration in the Amur river during 1995–1997

Yuto Tashiro[1*], Tetsuya Hiyama[1], Hironari Kanamori[1] and Masayuki Kondo[1,2]

Abstract

Primary production in the Sea of Okhotsk is largely supported by dissolved iron (dFe) transported by the Amur river, indicating the importance of dFe discharge from terrestrial environments. However, little is known about the mechanisms of dFe discharge into the Amur river, especially in terms of long-term change in dFe concentration. In the Amur river, extreme increase in dFe concentration was observed between 1995 and 1997, the cause of which remains unclear. As a cause of this iron anomaly, we considered the impact of permafrost degradation. To link the permafrost degradation to long-term variation in dFe concentration, we examined the changes in annual air temperature (Ta), accumulated temperature (AT), and net precipitation for three regions (northeast, south, and northwest) of the basin between 1960 and 2006. Ta and AT were relatively high in one out of every few years, and were especially high during 1988–1990 continuously. Net precipitation in late summer (July to September) has increased since 1977 and has stayed positive until 2006 throughout the basin. Most importantly, we found significant correlations between Ta and late summer dFe concentration with a 7-year lag ($r = 0.54–0.69$, $p < 0.01$), which indicate a close relationship between high Ta in year Y and increased late summer dFe concentration in year Y + 7. This correlation was the strongest in northeastern Amur basin where permafrost coverage is the highest. Similar 7-year lag correlation was also found between AT in the northeastern basin and late summer dFe concentration ($r = 0.51$, $p < 0.01$). Based on our findings, we propose the following hypothesis as a cause of iron anomaly. (1) Increased net precipitation since 1977 has increased soil moisture, which created suitable conditions for microbial dFe generation; (2) permafrost degradation during the warm years of 1988–1990 promoted iron bioavailability and led to the intensive dFe generation in the deeper part of the active layer; and (3) dFe took approximately 7 years to reach the rivers and extremely increased dFe concentration during 1995–1997. This is the first study to suggest the time-lagged impact of permafrost degradation on iron biogeochemistry in the Amur river basin.

Keywords Amur river, Dissolved iron, Permafrost, Climate change, Pacific decadal oscillation

*Correspondence:
Yuto Tashiro
tassy40y@gmail.com
Full list of author information is available at the end of the article

1 Introduction

Iron is an important trace element for living organisms. It is involved in numerous in vivo metabolic processes, including photosynthetic electron transport, respiration, and N_2-fixation (Sunda 2012). The bioavailability of dissolved iron (dFe) often limits biological productivity in world oceans, especially in high-nutrient low-chlorophyll regions (Bruland and Lohan 2003; Martin and Fitzwater 1988; Martin et al. 1989, 1990, 1994; Price et al. 1994; Takeda and Obata 1995). Aeolian dust input was previously considered to be the critical source of iron for the ocean (Martin and Fitzwater 1988). However, many studies have indicated that land-derived dFe input by rivers is also important for primary production in coastal areas and open sea areas (Krachler et al., 2010, 2016, 2021; Laglera and Van Den Berg 2009; Matsunaga et al. 1998; Moore and Braucher 2008; Nishioka et al. 2013, 2014). Against this background, a considerable number of studies have recently been made on the sources and overlook of dFe in terrestrial environments (Ilina et al. 2013; Ingri et al. 2018; Kritzberg and Ekström, 2012; Palviainen et al. 2015; Sarkkola et al. 2013).

The Sea of Okhotsk has abundant marine resources, and its abundance is among the highest in the world (Sorokin and Sorokin 1999). Its high biological productivity is partly a result of the abundant dFe derived from the forests and wetlands in the Amur river basin (Nishioka et al. 2013, 2014; Shiraiwa 2012; Suzuki et al. 2014). According to the previous studies, the extensive wetlands in the lower Amur basin and the permafrost wetlands in the middle Amur basin are important sources of dFe for the Amur river (Nagao et al. 2007; Wang et al. 2012; Tashiro et al. 2020, 2023). However, little is known about the mechanisms of dFe discharge into the Amur river, especially in terms of long-term changes in dFe concentration. The largest increase in dFe concentration in the Amur river was recorded between 1995 and 1997; this phenomenon was also observed in the tributaries and is referred to as the iron anomaly by Shamov et al. (2014). Because air temperature in the Amur river basin has increased since the mid-1980s to the early 1990s and remained high during 1990s (0.75℃ higher than the mean of 1960–1990) (Novorotskii 2007), Shamov et al. (2014) indicated the possibility that permafrost degradation promoted iron bioavailability in the deeper part of the active layer, which is the soil layer that is subjected to seasonal freeze–thaw dynamics, leading to microbial iron reduction under anaerobic conditions and subsequent increase in dFe discharge from soil to river. This hypothesis is partially supported by recent studies, which have reported relatively high dFe or aqueous Fe(II) concentrations in the deep part of the active layer in summer (Herndon et al. 2015; Jessen et al. 2014). Tashiro et al. (2020) also observed that seasonal soil thawing changes the source of dFe to rivers from the surface to deep soil layer in permafrost watersheds in the Amur river basin. If permafrost degradation is the main cause of iron anomaly during 1995–1997, increased dFe concentration should have been observed after summer when deep groundwater (suprapermafrost water) more contributes to river water. However, Shamov et al. (2014) have overlooked the seasonal variation in dFe concentration in the Amur river, and moreover, there has been no evidence supporting the relationship between warming-induced permafrost degradation and extremely increased dFe concentration in the Amur river between 1995 and 1997. Therefore, the mechanisms underlying the iron anomaly still remain unclear. If permafrost degradation has a large impact on iron biogeochemistry in the Amur river Basin, dFe concentration in the Amur river might change considerably under a warmer climate in the future and influence the marine ecosystem of the Sea of Okhotsk.

Over the past few decades, impacts of permafrost degradation on Arctic river biogeochemistry have been the subject of intense controversy (Colombo et al. 2018; Frey et al. 2009). Many studies have been conducted to reveal the temporal patterns of different aspects of water chemistry, including carbon, nutrients, and metals in the Siberian regions (Kawahigashi et al. 2004; Pokrovsky et al. 2015, 2016; Vorobyev et al. 2017, 2019) and the North American Arctic regions (Aiken et al. 2014; Frey et al. 2007; Kokeji and Burn 2005; Olefeldt et al. 2014; Petrone et al. 2006). Following these studies, it is now widely accepted that permafrost degradation shifts water flow paths to greater depths and changes biogeochemical cycles in watersheds. For example, the decrease in dissolved organic carbon (DOC) flux in the Yukon river in the past few decades has been attributed to the shifting of water flow paths from the upper organic-rich layer to the deeper mineral horizon where DOC can be adsorbed on soil particles (Striegl et al. 2005). Similarly, some studies have analysed multi-decadal water chemistry monitoring data and reported long-term changes in Arctic biogeochemistry; these include a decrease in DOC and increases in Ca, Mg, Na, P, and SO_4 in the Yukon river (Striegl et al. 2005; Toohey et al. 2016), increases in Ca, Mg, SO_4, and HCO_3 in Central Siberian rivers (Kolosov et al. 2016), increases in alkalinity in the Ob and Yenisei rivers (Drake et al. 2018), increase in NO_3 and decrease in DOC in the Kuparuk river in Alaska (McClelland et al. 2007), and increases in DOC and alkalinity in the Mackenzie river (Tank et al. 2016). These studies demonstrate the value of long-term river water chemistry monitoring in contributing to our understanding of the multi-decadal changes in Arctic biogeochemistry. However, it should be noted that monitoring data are generally

collected near the river mouth and include information on the total biogeochemical changes of the entire basin. Therefore, it is difficult to link permafrost degradation in specific regions of the basin to long-term changes in water chemistry by examining only monitoring data. To better understand the impact of climate change on biogeochemical cycles using long-term water chemistry monitoring data, changes in regional (basin) scale climate variables, such as air temperature and precipitation, need to be identified, and the relationship between these changes and observed changes in river water chemistry should also be analysed.

In this study, we analysed long-term monitoring data of dFe concentration and atmospheric reanalysis data from the Amur River basin from 1960 to 2006 to evaluate that warming-induced permafrost degradation was responsible for the extreme increase in dFe concentration between 1995 and 1997. We (1) examined the correlation between the long-term changes in dFe concentration and climate variables (specifically, air temperature and net precipitation); and (2) proposed a detailed hypothesis about the causes and mechanisms underlying the iron anomaly. The main study focus is the influence of climate change and permafrost degradation on the biogeochemical iron cycle in the Amur River basin. Our discussion also includes hydroclimatology and the importance of integrating climate data analyses into studies of the long-term changes in Arctic and sub-Arctic river biogeochemistry.

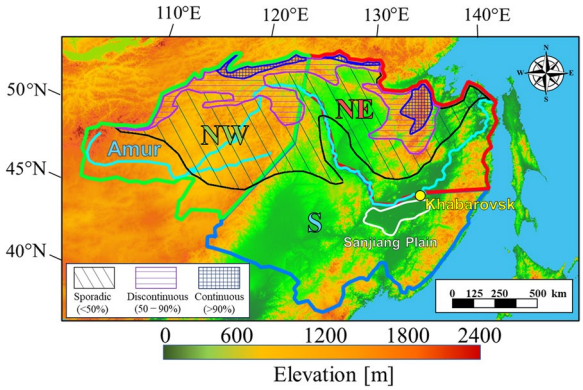

Fig. 1 Topographic map of the Amur River basin. The northeastern (NE-Amur), northwestern (NW-Amur), and southern (S-Amur) study regions are enclosed by the red, green, and blue lines, respectively. Long-term monitoring of dissolved iron (dFe) concentration and discharge was conducted at Khabarovsk station (yellow dot). Area enclosed white line shows Sanjiang Plain where large-scale agricultural developments were conducted in twentieth century (see discussion 3.3). Shading areas denote different types of permafrost distribution, which was created by authors with reference to Shamov et al. (2014)

2 Methods

2.1 Study site

The Amur River basin covers a large area (approximately 1.86 million km^2) in eastern Eurasia; it includes eastern Mongolia and forms the border between the Russian Far East and northeastern China. The Amur River transports large quantities of freshwater to the Sea of Okhotsk and is responsible for more than half of the total river inflow to the Sea of Okhotsk.

Climate variability in the Amur River basin largely varies by regions. Annual precipitation ranges from 300 mm in eastern Mongolia to more than 700 mm in the Russian Far East and northeastern China. The annual mean of air temperature also ranges from around 6 °C in the south to − 7 °C in the north. Therefore, we analysed the climate data for three regions of the Amur River basin: northwestern Amur (NW-Amur), southern Amur (S-Amur), and northeastern (NE-Amur) (Fig. 1). The NE-Amur lies mainly to the north of the Amur River and is dominated by taiga forests and lowland wetlands. Most of the NE-Amur is in isolated (< 10% coverage) and sporadic (10–50%) permafrost zones. In contrast, the S-Amur has almost no permafrost, and a considerable fraction of the region is occupied by agricultural land. The NW-Amur includes the uppermost part of the Amur River, and is also the driest of the three regions. The northern and eastern parts of the NW-Amur are in a sporadic permafrost zone dominated by taiga forests, while the southwestern part of the NW-Amur, which forms part of the Mongolian Plateau, is in a dry steppe zone without permafrost.

2.2 Data from the monitoring of dFe in the Amur River

Concentration of dFe in the Amur River was monitored at Khabarovsk station of the Federal Service for Hydrometeorology and Environmental Monitoring of Russia (Roshydromet) from 1960 to 2006 (Fig. 1). Water was sampled once a month between April and October and on a few occasions between November and March. River discharge on the sampling day was also measured at the same station. Dissolved iron was measured by the colorimetric method with 1,10-phenantroline, which was applied to water filtered through Whatman GF/F filters (0.7 μm) and acidified to pH < 2 with HCl (Hydrochemical Institute 2006).

As described in the introduction, seasonal soil thawing has a great influence on water path and riverine dFe concentration in permafrost watersheds in the Amur River basin. To improve our understanding of the mechanisms underlying the iron anomaly, seasonal changes in iron dynamics should be considered; therefore we analysed not only the interannual variations of dFe concentrations, but also the seasonal mean dFe concentrations.

We defined April, May, and June (AMJ) as late spring and July, August, and September (JAS) as late summer. River characteristics are dominated by snowmelt in late spring, especially from late April to June, and by rain in late summer, especially in July and August; active layer thickness peaks in September (Tashiro et al. 2020).

2.3 Climate data analyses

For the three regions, we investigated the interannual variations in annual air temperature (Ta) for 1960–2006 using the data from the Climatic Research Unit gridded Time Series v4.05 (CRU) on a 0.5° latitude/longitude grid (Harris et al. 2020). In addition, we investigated the interannual variations in accumulated temperature (AT) using 2-m surface air temperature data from the Japanese 55-year Reanalysis Project (JRA-55), which is on a 1.25° latitude/longitude grid (Kobayashi et al. 2015). We calculated annual AT, which is the cumulative sum of the regional mean daily average temperature above 0 °C in a year; AT is commonly used as an index of maximum active layer thickness (Hinkel et al. 2001). Additionally, we investigated the interannual variations in mean air temperature in late summer (JAS) using the data from JRA-55 to evaluate the contribution of air temperature in late summer to AT. Note that we confirmed good agreement between interannual variations in Ta calculated from CRU and those calculated from JRA-55 (Additional file 1: Fig. S1), therefore we decided to use Ta from CRU for the following analyses because CRU reflects the observation data from meteorological stations more directly than JRA-55.

We also calculated the interannual variations in net precipitation (precipitation minus evapotranspiration: P − E) in late summer (JAS) for 1960–2006. Late summer P − E indicates the net recharge of water in the soil layer. It is a useful indicator of the long-term trends in soil moisture and groundwater discharge to rivers, which can be related to iron redox reactions in soils and subsequent dFe discharge. For calculating P − E, we used the atmospheric water budget equation (Peixoto and Oort 1983, 1992):

$$P - E = C - \partial W/\partial t, \quad (1)$$

where P is precipitation, E is evapotranspiration, C is the vertically integrated (from the ground to the 100-hPa) moisture flux convergence, and $\partial W/\partial t$ is the temporal change in the precipitable water. Because $\partial W/\partial t$ over long periods of more than one month is small compared with P − E and C, $\partial W/\partial t$ is considered as negligible for calculating mean P − E in late summer. We calculated the C from specific humidity, zonal and horizontal winds of the JRA55 dataset.

Wet or dry period in land can change over decadal scale due to the natural variability of the atmosphere (Liu et al. 2022). The atmospheric circulation pattern in the Amur River basin is closely associated with the Pacific Decadal Oscillation (PDO) (Mokhov and Semenov 2016). To understand the background of periodic change in late summer P − E (wet or dry tendency) in the Amur River basin, which can be important for iron dynamics, we investigated the relationship between late summer P − E and those in the mean late summer PDO index. The PDO is a long-term oscillation of the Pacific Ocean on time scales of approximately 20–30 years (Mantua et al. 1997). The PDO index is an indicator of the PDO and is defined as the projections of monthly mean sea surface temperature (SST) anomalies onto their first empirical orthogonal functions (EOF) vectors in the North Pacific (north of 20° N). When the PDO index is positive (negative), SSTs in the central part of the North Pacific are likely to be lower (higher) than normal. During our study period (1960–2006), the PDO was in a positive phase between 1977 and 1997. We obtained monthly PDO index data from Japan Meteorological Agency (https://www.data.jma.go.jp/gmd/kaiyou/data/shindan/b_1/pdo/pdo.html) and conducted two-tailed tests of significance for the Pearson's correlation coefficients between the 9-year moving averages of late summer P − E and those of the PDO index for 1960–2006. In general, moving average within 10 years is applied to the interannual variation in the PDO index (e.g. Zhang et al. 2020), and we confirmed that 9-year moving average maximized the correlation between late summer P − E and the PDO index compared to 3-, 5-, and 7-year moving averages.

To better understand the periodic changes in late summer P − E in the Amur River basin associated with PDO phase change, we focused on the characteristics of the atmospheric conditions during the positive phase of the PDO between 1977 and 1997. We used JRA55 data to calculate the anomaly of the mean geopotential height at the 500-hPa level in late summer in 1977–1997 from 1960 to 2006 means (Z_{500}) and the anomaly of mean vertically integrated water vapour flux in 1977–1997 from 1960 to 2006 means. Because positive (negative) P − E means convergence (divergence) of water vapor, the anomaly of Z_{500} will exhibit the appearance of cyclonic (anticyclonic) circulation patterns which enhances (suppresses) the water vapor convergence and divergence. In addition, the anomaly of vertically integrated water vapor flux will allow us to understand the change in transport of water vapor flux associated with cyclonic and anticyclonic circulation patterns.

2.4 Statistical analyses

We conducted cross correlation analyses of the interannual variations in annual, late spring, and late summer dFe concentration in the Amur River and climate variables (Ta and P − E) in the NE-Amur, the NW-Amur, and the S-Amur. We used time lags of 0–9 years because soil permeability is low and it would take several years for changes in Ta and P − E to affect dFe discharge through permafrost degradation in the deeper part of the active layer (Quinton et al. 2008, 2009; Shamov et al. 2014). We calculated Pearson's correlation coefficients as indicators of the strength of the association between the variables and conducted two-tailed tests of significance (n = 46, 45, 44, 43, 42, 41, 40, 39, 38, 37 for time lags of 0, 1, 2, 3, 4, 5, 6, 7, 8 and 9 years, respectively).

3 Results and discussion

3.1 Changes in climate variables in the Amur River basin between 1960 and 2006

Interannual variations in Ta in the NE-Amur, the NW-Amur, and the S-Amur between 1960 and 2006 exhibited similarities (Fig. 2a). Average Ta between 1960 and 2006 was − 3.1 °C in the NE-Amur, − 2.8 °C in the NW-Amur, and 1.6 °C in the S-Amur. The iron anomaly occurred between 1995 and 1997; for this period, Ta was not particularly high in the three regions. Between 1960 and 2006, Ta was relatively high in one out of every few years, for example in 1963, 1968, and 1975. In particular, high Ta was maintained for three years between 1988 and 1990 throughout the entire Amur River basin, with 1990 being the warmest year between 1960 and 2006 in the NE-Amur (Ta was − 1.5 °C in 1990) and S-Amur (Ta was 2.8 °C in 1990). The interannual variations in AT in the three regions were similar to those of Ta; AT was relatively high in the years with high Ta in 1963, 1968, 1975, and 1988–1990 (Fig. 2b). During the continuous warm years of 1988–1990, the highest AT in the NE-Amur between 1960 and 2006 was shown in 1988 (AT in 1990 in this region was also relatively high). In addition, the interannual variations in AT were significantly correlated with those in late summer air temperature (Additional file 1: Figs. S2 and S3), indicating that high air temperature in late summer largely contributes to high AT. For example, in 1988 with the highest AT between 1960 and 2006, late summer air temperature in the NE-Amur was 15.5 °C, which was 1.4°C higher than the mean of 1960–2006 (Additional file 1: Fig. S2). Given that AT can be an index of maximum active layer thickness (Hinkel et al. 2001), continuous high AT between 1988 and 1990 indicates considerable acceleration of permafrost degradation in the NE-Amur. These results are in agreement with long-term soil temperature monitoring data from weather stations in sporadic permafrost zones in the NE-Amur (Shamov et al. 2014); the data showed large increases in soil temperature between 1988 and 1990.

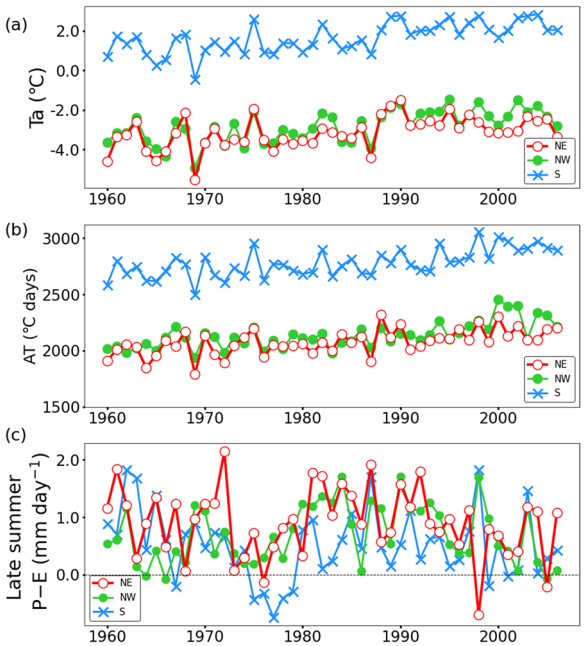

Fig. 2 Interannual variations of climate variables in the Amur River basin. Regional mean **a** annual air temperature (Ta), **b** accumulated temperature (AT), and **c** late summer (July, August, September; JAS) mean net precipitation (P − E) in the NE-Amur (red), the NW-Amur (green), and the S-Amur (blue). In **c**, P − E values above the black dotted line indicate net water gain as a result of infiltration and values below the line indicate net water loss as a result of evapotranspiration

Interannual variations of late summer P − E in the NE-Amur, the NW-Amur, and the S-Amur also exhibited similar patterns (Fig. 2c). In particular, late summer P − E in the Amur River basin had clear interdecadal variations. In the three regions, P − E decreased after 1960; after around 1977, P − E increased and remained positive and high until around 1990, and then decreased to 2006. Increased P − E suggests that net water infiltration into the soil in the Amur River basin increased after 1977 (after 1980 for the S-Amur) and these conditions of increased soil moisture remained until 2006 throughout the basin. In particular, P − E in the NE-Amur and the NW-Amur has been higher than that in the S-Amur since 1977; this result suggests that soil moisture increases in the northern parts of the Amur River basin have been larger than those in the southern regions. It should be noted that negative late summer P − E with large magnitudes was found in the NE-Amur in 1998. In the NE-Amur, 1998 is known as an anomalous drought year and is associated with historic catastrophic forest fires in the Khabarovsk Krai (Sokolova et al. 2019).

We also found that 9-year moving averages of late summer P − E in the NE-Amur and NW-Amur were significantly correlated with those of the late summer PDO index for 1960–2006 (NE-Amur: $r^2 = 0.38$, $p = 2{,}31 \times 10^{-5}$; NW-Amur: $r^2 = 0.92$, $p = 1.53 \times 10^{-22}$) (Fig. 3a). In 1977, the PDO switched from negative to positive phase and remained positive until 1997. These results suggest that the increase in P − E after 1977 was related to the PDO phase change. Examination of Z_{500} during the positive phase of the PDO (1977–1997) reveals an anticyclonic anomaly around the Sea of Okhotsk, and a cyclonic anomaly around the NW-Amur (Fig. 3b). These results are in close agreement with those from Zhang et al. (2020), which showed the presence of anticyclonic and cyclonic wave-like teleconnection pattern in the midlatitudes of the Northern Hemisphere during the positive PDO phase. In addition, the anomaly of the vertically integrated water vapour flux during 1977 − 1997 showed increases in eastward water vapour flux into NE-Amur and NW-Amur and northward water vapour flux into the coastal area of NE-Amur and S-Amur. On the basis of these results, we infer that the increase in late summer P − E in the Amur River basin after 1977 (Fig. 2b), especially in the NE-Amur and NW-Amur, was likely a result of the changes in the atmospheric circulation pattern associated with the positive phase of the PDO of 1977–1997.

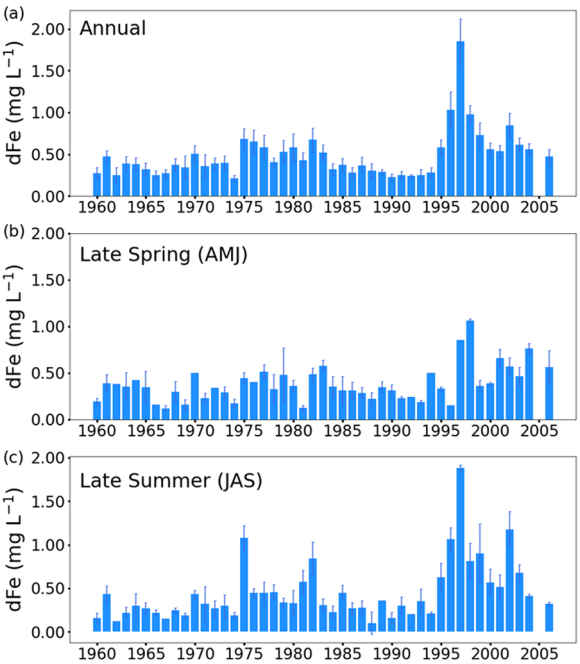

Fig. 4 Interannual variations in annual/seasonal dissolved iron (dFe) concentrations in the Amur River. **a** Annual, **b** late spring (April, May, June; AMJ), and **c** late summer (July, August, September; JAS) mean dFe concentrations. Error bars show the standard error of the data. Data from 2005 are missing

3.2 Lag relationship between the interannual variations in climate variables and dFe concentration in the Amur River basin

Figure 4 shows the interannual variations in annual/seasonal dFe concentrations in the Amur River. The range of annual concentration variations remained small between 1960 and 1994. Between 1995 and 1997, there was an extremely large increase in annual concentration (Fig. 4a). The peak of annual concentration in 1997 was 1.85 mg L^{-1}, which was approximately 500% of the mean concentration (0.38 mg L^{-1}) of 1960–1994. There were similar variations in late summer concentration (Fig. 4c). There was an extremely large increase in late summer

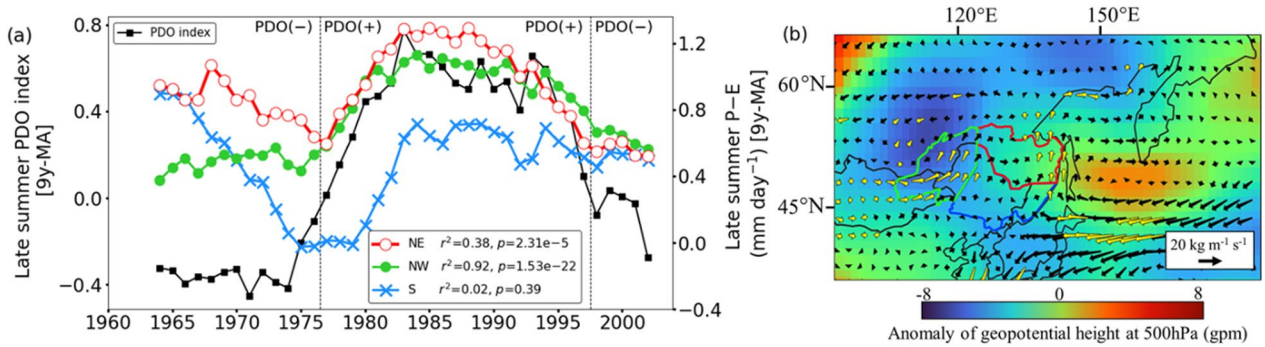

Fig. 3 Changes in late summer net precipitation (P − E), Pacific Decadal Oscillation (PDO) index, and atmospheric circulation. **a** Interannual variations in the 9-year moving averages of late summer (July, August, and September; JAS) P − E in the NE-Amur (red), the NW-Amur (green), the S-Amur (blue), and late summer PDO index (black); **b** the anomaly of mean geopotential height at the 500-hPa level in late summer during the positive PDO phase of 1977–1997 relative to 1960–2006. In **a**, the black dotted two lines indicate the years 1977 and 1997, when the phase of the PDO changed from negative (positive) to positive (negative). In **b**, the red area indicates the high-pressure anomaly, while the blue area indicates the low-pressure anomaly. Arrows denote the anomaly of mean vertically integrated water vapour flux during 1977–1997 relative to 1960–2006. Yellow arrows denote that the anomaly was statistically significant at the 95% confidence level in *t*-tests

concentration between 1995 and 1997; the peak in 1997 was 1.88 mg L^{-1}, which was approximately 600% of the mean concentration (0.33 mg L^{-1}) of 1960–1994. There was an extremely large increase in late spring concentration between 1997 and 1998 (Fig. 4b), which was 1 year after the extreme increase in annual and late summer concentrations. The peak of late spring concentration in 1998 was 1.06 mg L^{-1}, which was lower than the peak of late summer concentration (1.88 mg L^{-1}) in 1997.

Cross correlation coefficients between annual/seasonal dFe concentrations and climate variables (Ta, AT, and late summer P − E) are shown in Fig. 5. No significant correlation was found between annual/seasonal concentrations and late summer P − E at lags of 0–9 years (Fig. 5g–i). For Ta, the strongest significant positive correlation was found between annual dFe concentration and Ta at a lag of 7 years (NE-Amur: $r=0.55$, $p=0.0003$; NW-Amur: $r=0.43$, $p=0.0059$; S-Amur: $r=0.49$, $p=0.0016$), and the second strongest correlation was found at a lag of 8 years (NE-Amur: $r=0.48$, $p=0.0021$; S-Amur: $r=0.44$, $p=0.0052$) (Fig. 5a). Similarly, there was a significant positive correlation between late summer dFe concentration and Ta at a lag of 7 years (NE-Amur: $r=0.69$, $p=1.4\times10^{-6}$; NW-Amur: $r=0.54$, $p=0.0004$; S-Amur: $r=0.60$, $p=5.7\times10^{-5}$) (Fig. 5c). Correlation coefficients between late summer dFe concentrations and Ta exceeded those between annual concentrations and Ta. It is noteworthy that correlation coefficients between annual/late summer dFe concentration and Ta with a lag of 7 years were the largest in the NE-Amur, where permafrost is sporadically distributed. These results indicate a close relationship between high Ta in NE-Amur in year Y and increased annual/late summer dFe concentrations in the Amur River in year Y + 7. Figure 6a shows the scatter plot of late summer dFe concentration and Ta in NE-Amur with a lag of 7 years. The lag of 7 years can also be found by comparing the interannual variations in Ta and late summer dFe concentration; in NE-Amur, Ta was relatively high in 1963, 1968, 1975, 1988–1990, and 1995 (Fig. 2a), and late summer dFe concentration increased in 1970, 1975, 1982, 1995–1997, and 2002 (Fig. 4c). There is a similar lag relationship between annual/seasonal dFe concentrations and AT in the NE-Amur (Fig. 5d–f) and the largest correlation coefficient was found between late summer concentrations and AT with a lag of 7 years ($r=0.51$, $p=0.0010$) (Fig. 5f). This implies that late summer dFe concentration in the Amur River increased 7 years after the acceleration of permafrost degradation because of warm summer in the NE-Amur.

For late spring dFe concentration, the strongest significant positive correlation was found between late spring concentration and Ta at a lag of 9 years (NE-Amur:

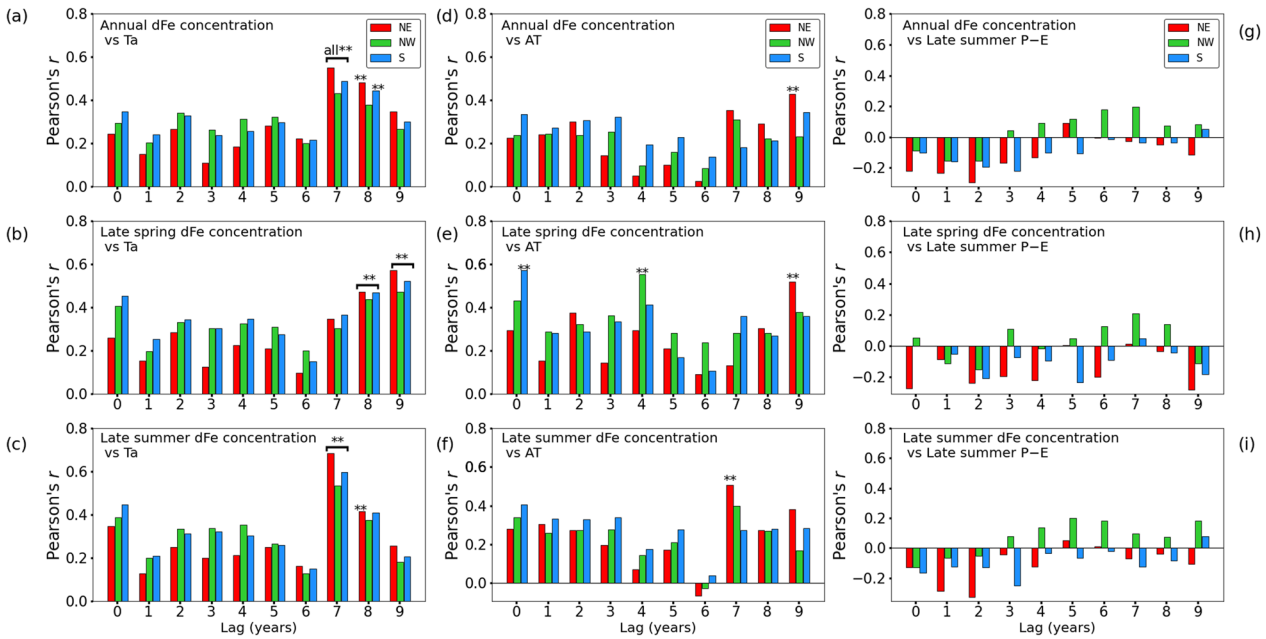

Fig. 5 Cross correlation coefficients between dissolved iron (dFe) concentrations and climate variables in the Amur River basin. **a** Annual dFe concentrations and mean air temperature (Ta); **b** late spring (April, May, June; AMJ) dFe concentrations and Ta; **c** late summer (July, August, September; JAS) dFe concentrations and Ta; **d** Annual dFe concentrations and accumulated temperature (AT); **e** late spring dFe concentrations and AT; **f** late summer dFe concentrations and AT; **g** annual dFe concentrations and late summer net precipitation (P − E); **h** late spring dFe concentrations and late summer P − E; **i** late summer dFe concentrations and late summer P − E. In **a**–**c**, ** indicates $p<0.01$

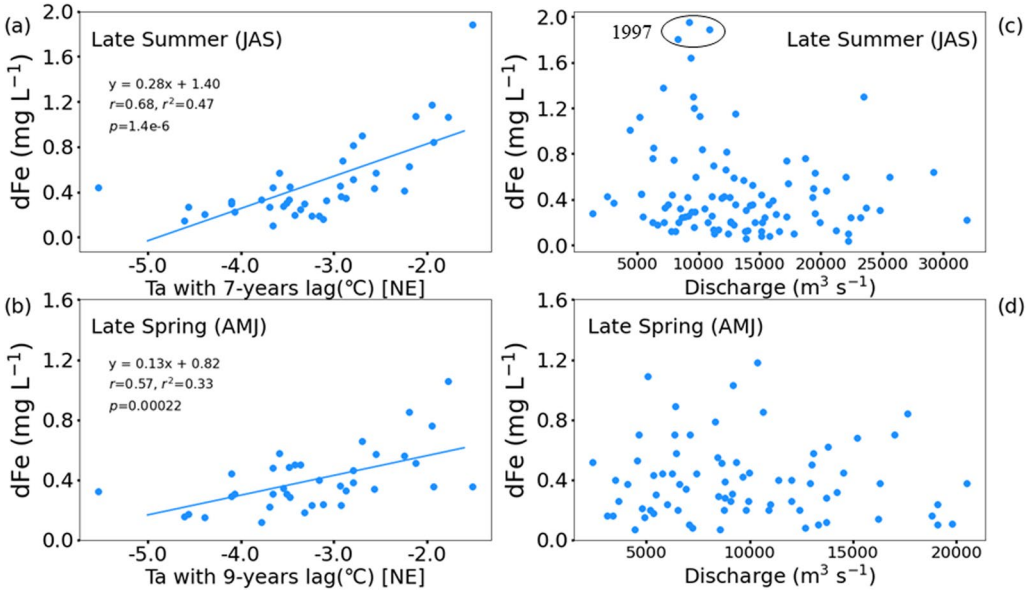

Fig. 6 Relationship between dissolved iron (dFe) concentrations, time lagged annual air temperature (Ta), and discharge. **a** Late summer (July, August, and September; JAS) dFe concentrations in the Amur River and Ta with a 7-year lag in the NE-Amur; **b** late spring (April, May, and June; AMJ) dFe concentrations and Ta with a 9-year lag in the NE-Amur; **c** late summer dFe concentrations and discharge; **d** late spring dFe concentrations and discharge. Only Ta in the NE-Amur is shown because the Pearson's coefficient between Ta and dFe in the NE-Amur is higher than that in NW-Amur and that in S-Amur (Fig. 5a–c). In **a** and **b**, seasonal mean dFe concentrations are shown. In **c** and **d**, individual measurements of dFe concentration and discharge are shown. In **c**, the black circle denotes the data in 1997, which is the peak year of iron anomaly

$r=0.57$, $p=0.0002$; NW-Amur: $r=0.47$, $p=0.0033$; S-Amur: $r=0.52$, $p=0.0009$) and the second strongest correlation was found at a lag of 8 years (NE-Amur: $r=0.47$, $p=0.0027$; NW-Amur: $r=0.44$, $p=0.0061$; S-Amur: $r=0.47$, $p=0.0030$) (Fig. 5b). Similar to annual/late summer dFe concentrations, correlation coefficients between late spring concentration and Ta with a lag of 9 years in the NE-Amur were larger than those for NW-Amur and S-Amur. Figure 6b shows the significant positive correlation between late spring dFe concentration and Ta in NE-Amur with a lag of 9 years.

During a warm year, accelerated permafrost degradation produces thawed soil; Fe(III) minerals in the newly thawed soil can be exposed to microbial reduction, which could lead to the intensive generation of soluble Fe(II) in the soils that are deep in the active layer. Studies have confirmed the accumulation of dFe and dissolved Fe(II) in the deeper part of the active layer by investigating the vertical distributions of dFe and dissolved Fe(II) in permafrost areas in summer (Herndon et al. 2015; Jessen et al. 2014). The intensive generation of Fe(II) in deep soils can potentially increase riverine dFe concentration by forming complexes with humic substances, which are soluble in river waters with neutral pH (Laglera and Van Den Berg 2009). However, because soil permeability is low, the Fe(II) in deep soils will take several years to travel through the deeper part of the active layer to the rivers (Jessen et al. 2014; Quinton et al. 2008, 2009). Our results suggest that permafrost degradation in NE-Amur caused an intensive generation of Fe(II), which took approximately 7 years to reach rivers through the deeper soils in the active layer and subsequently increased dFe concentration in the Amur River. This is a plausible mechanism in terms of water path; deep groundwater (suprapermafrost water) considerably influences river water chemistry in late summer when active layer thickness reaches its maximum (Bagard et al. 2011; Evans et al. 2020). Given that the correlation coefficients between late summer dFe concentration and Ta were large for lags of 7 and 8 years, we infer that increased dFe discharge likely lasted for at least 1–2 years. Unexpectedly, we found a significant correlation between late spring dFe concentration and Ta at lags of 8 and 9 years (Fig. 5b and 6b), even though the influence of groundwater is minimum during spring floods. It is currently difficult to understand the difference between the 7- and 8-year lag in late summer and the 8- and 9-year lag in late spring, but these higher dFe concentrations in late spring may be related to increased dFe discharge in late summer. One possible mechanism could be that deep groundwater-derived dFe partially precipitated as iron-oxyhydroxides after flowing into the river in late summer, and dissolved again the following spring when it came into contact with the large amounts of DOC that were released from the organic-rich topsoil

by snowmelt. Another possible mechanism is that deep groundwater is not fully frozen and continues to interact with river waters even in spring.

In addition to inflow of dFe-rich groundwater, seasonal hydrological events are well known to greatly influence on riverine dFe concentration in the Amur River basin (Tashiro et al. 2020; Yan et al. 2016). Tashiro et al. (2020) observed seasonal variation in dFe concentration in the Amur-Mid region (central part of the NE-Amur) and found that spring snowmelt and summer rainfall greatly contributes to dFe runoff into rivers from organic soil layer. Increased dFe concentration during spring floods was also observed in the Amur River and tributary in the S-Amur (Yan et al. 2016). In general, increases in dFe concentration in response to hydrological events such as summer rainfall and spring snowmelt are observed simultaneously with increased water level and discharge in the Arctic and sub-Arctic regions (Abesser et al. 2006; Anderson et al. 2006; Tashiro et al. 2020; Rember and Trefry 2004). However, we found no significant correlation between the individual measurements of Amur River discharge and late spring/late summer dFe concentration (Fig. 6c–d). Therefore, interannual variations in annual/seasonal dFe concentrations in the Amur River between 1960 and 2006, including the iron anomaly (1995–1997), were not fully explained by the impacts of snowmelt and rainfall.

3.3 Mechanisms underlying the iron anomaly between 1995 and 1997

It should be emphasized that the iron anomaly between 1995 and 1997 was a widespread phenomenon, which was observed in many of the tributaries in the NE-Amur (Shamov et al. 2014). Based on this fact and the 7-year lag between Ta, AT and late summer dFe concentration (Fig. 3b,e), we hypothesize that the extreme increase in dFe concentration in the Amur River between 1995 and 1997 was resulted from accelerated permafrost degradation caused by continuous warming between 1988 and 1990 in the NE-Amur (Fig. 2a). In particular, 1988 was the warmest spring–summer between 1960 and 2006 in the NE-Amur, as shown in interannual variation in AT (Fig. 2b). Actually, late summer air temperature in 1988 in the NE-Amur was 15.5℃, which was 1.4 °C higher than the mean of 1960–2006 (Additional file 1: Fig. S2). Although the peaks of AT and late summer air temperature were shown in 1988, the steady increases in soil temperature by approximately 1.0℃ were recorded at several weather stations in the NE-Amur from 1988 to 1990 (Shamov et al. 2014). As discussed in the previous section, accelerated permafrost degradation followed by the increased soil temperature in these years may have caused the iron anomaly in the Amur River between 1995 and 1997 by the inflow of dFe-rich groundwater through the deeper part in active layer. In terms of permafrost hydrology, this mechanism is in good agreement with the fact that the highest dFe concentration (2.75 mg L^{-1}) in 1997, the peak year of iron anomaly, was observed in October when the contribution of deep groundwater to rivers increases as the active layer thickness reaches its maximum. Moreover, previous study on long-term record of iron content in the Amur River during the winter low water level showed that the highest dFe discharge (269 t day^{-1}) was observed in 1995–1996 winter, which was considerably higher than the mean of 1950–2012 (47.7 t day^{-1}) (Shesterkin et al. 2013). There was unfortunately no available data of dFe concentration, and winter observation for 1996–1997 and 1997–1998 were missing in the previous study. Nevertheless, their results support our hypothesized mechanism that the iron anomaly between 1995 and 1997 was caused by the inflow of dFe-rich groundwater because winter baseflow is generally dominated by deep groundwater rich in minerals (Bagard et al. 2011; Holmes et al. 2012).

Increased late summer P − E after 1977 in the Amur River basin (Fig. 2c), which is likely resulted from increased water vapour flux convergence during the positive PDO phase (1977–1997) (Fig. 3), could have also promoted dFe discharge into the Amur River. Although we found no significant relationship between annual/seasonal dFe concentrations and late summer P − E (Fig. 5g–i), we hypothesize that persistently positive P − E after 1977 throughout the Amur River basin may have had the following effects on the biogeochemical and hydrological cycles: (1) intensification of permafrost degradation because of increased water infiltration and increased heat transport to deeper soil (Douglas et al. 2020); (2) promotion of microbial iron reduction under anaerobic conditions because of increased soil water content (Lipson et al. 2012); and (3) increased groundwater discharge into rivers (Connon et al. 2014). These effects were likely more intense in the NE-Amur and the NW-Amur, where late summer P − E were larger than those in the S-Amur after 1977 (Fig. 2c).

The relative importance of dFe transport from the NE-Amur to the Amur River is also supported by the differences in the water chemistry of the tributaries in the three regions. According to previous studies on the distribution of riverine dFe concentration in the middle and lower Amur River basin, the amount of dFe, humic acids, and organically-bound Fe is much higher in rivers in the NE-Amur than in the S-Amur because of the large amounts of organic matter and humic substances in the taiga forests and lowland wetlands in the NE-Amur (Levshina et al. 2012, 2016). Unfortunately, there is no report on riverine dFe concentration in the NW-Amur, but it is

supposed to be low because of the low concentrations of DOC and humic substances in the rivers in this region (Levshina et al. 2016). Taking into account these regional characteristics of the river water chemistry in the Amur River basin, we infer that the NE-Amur has the highest dFe supply capacity in the basin. In addition, Tashiro et al. (2020) examined the seasonal variations in dFe concentrations in peat soils and rivers and concluded that wetlands (peat bogs) with underlying permafrost in the NE-Amur can be important sources of dFe to the Amur River. Combining the findings from previous studies and those from the present study, we infer that increased dFe discharge from permafrost-distributed landscapes such as wetlands (Tashiro et al. 2020, 2023) in the NE-Amur were the primary causes of the extreme increase in dFe concentration between 1995 and 1997.

In addition to permafrost degradation, land use change may have a considerable influence on dFe concentration. According to Ganzey et al. (2010), the areas of forests and wetlands in the NE-Amur remained almost unchanged between 1930 and 2000, except for the northern part of Sikhote-Alin (Fig. 1) where intensive deforestation was carried out in the 1980s. In contrast, large-scale agricultural developments have taken place in the Sanjiang Plain in the S-Amur in the twentieth century (Fig. 1). Between 1949 and 1994, 72.2% of the wetland area (approximately 4 Mha) was reclaimed and converted to paddy fields (Pan et al. 2011). This had considerable impacts on riverine dFe concentration in the Sanjiang Plain. For example, the Naoli River in the Sanjiang Plain showed a steady decrease in the concentration of free iron because of an 87% decrease in wetlands in the watershed between 1949 and 2000 (Pan et al. 2011). On the contrary, using Fe(II)-rich groundwater to irrigate paddy fields may increase dFe discharge into rivers through agricultural canals. However, the impact of irrigation on dFe discharge is likely to be small. Previous study showed that more than half of the dFe precipitates during irrigation because of the low concentration of organic ligands such as humic acids in the paddy fields of Sanjiang Plain (Pan et al. 2011). According to numerical modelling studies, groundwater pumping is estimated to increase the dFe flux from Sanjiang Plain by 2000 t year^{-1} (Onishi et al. 2009), which is only 3.4% of the extreme increase in dFe flux (58,400 t year^{-1}) in the Amur River in 1997 (Shamov et al. 2014). Therefore, we infer that land use change in the Amur River basin in twentieth century is clearly not the major cause of the iron anomaly.

Overall, we hypothesis that the extreme iron anomaly in the Amur River between 1995 and 1997 was resulted from continuous warming and permafrost degradation between 1988 and 1990 in the NE-Amur. Unfortunately, there is no multi-decadal monitoring data of dFe concentration from the tributaries of the Amur River. In addition, lack of knowledge of the detailed permafrost distribution and the mechanism of dFe discharge through the deeper part of the active layer precludes the verification of our 7-year lag hypothesis. Nevertheless, our results highlight the importance of studying the influence of permafrost degradation from a macroscopic perspective; long-term changes in Ta and late summer P − E, and these effects over time should be taken into consideration in the study of iron biogeochemistry in the Amur River basin. To improve our understanding of the iron anomaly, further research should be focused on permafrost distribution, soil profiles (peat and mineral horizons), soil permeability, and dFe dynamics in the deeper part of the active layer in the NE-Amur. Moreover, numerical modelling studies are also needed to validate the time lag relationships between Ta and the annual/seasonal dFe concentrations that were reported in this study.

4 Conclusions

In this study, we took the hydroclimatological approach to assess whether permafrost degradation is responsible for the extreme increase in dFe concentration in the Amur River during 1995–1997. After 1977, late summer P − E increased and remained positive and high throughout the basin, especially in the NE-Amur and NW-Amur. We inferred that increased soil moisture after 1977 was caused by increased water vapour flux convergence associated with the positive phase of the PDO (1977–1997). In the NE-Amur, spring-summers were considerably warm continuously between 1988 and 1990, and the highest AT was shown in 1988 between 1960 and 2006. More importantly, interannual variations in late summer dFe concentrations in the Amur River were significantly correlated with interannual variations in Ta and AT in the NE-Amur with a lag of 7 years. On the basis of these results, we propose the following hypothesis as a reasonable cause for the iron anomaly: continuous warming between 1988 and 1990 in the background of persistently higher levels of soil moisture since 1977 accelerated permafrost degradation in the NE-Amur and promoted iron bioavailability and dFe generation in the deeper part of the active layer; consequently, large amounts of dFe were discharged into rivers 7 years later, leading to an extreme increase in dFe concentration in the Amur River between 1995 and 1997. Further research is needed to verify our hypothesis. However, by taking a macroscopic perspective in this study, we discovered the significant time lag relationship between Ta, AT and dFe concentration. To our knowledge, this is the first study to suggest the time-lagged impact of permafrost degradation on iron biogeochemistry in the Amur River

basin, and to highlight the importance of the integration of climate data analyses into studies of Arctic and sub-Arctic river biogeochemistry with a focus on the influence of permafrost degradation.

Abbreviations

AT	Accumulated temperature
CRU	Climatic research unit
dFe	Dissolved iron
JRA-55	Japanese 55-year reanalysis
P − E	Precipitation minus evapotranspiration
PDO	Pacific decadal oscillation
Ta	Annual air temperature

Supplementary Information

The online version contains supplementary material available at https://doi.org/10.1186/s40645-024-00619-w.

Additional file 1. **Figure S1**. Relationship between annual air temperature (Ta) calculated from CRU and those from JRA-55 between 1960 and 2006 in the NE-Amur (red), the NW-Amur (green), and the S-Amur (blue). Black straight line denotes 1:1 line (y = x). **Figure S2**. Interannual variations in late summer (July, August, and September) air temperature in the NE-Amur (red), the NW-Amur (green), and the S-Amur (blue). **Figure S3**. Relationship between accumulated temperature (AT) and late summer air temperature in the NE-Amur (red), the NW-Amur (green), and the S-Amur (blue).

Acknowledgements
This research was funded by the Japan Society for the Promotion of Science (JSPS) KAKENHI (Grant Number 19H05668) project entitled "Pan-Arctic Water-Carbon Cycles (PAWCs)" (https://enpawcs.home.blog/). It was also supported by the Japan Science and Technology Agency (JST) Belmont Forum (Grant Number JPMJBF2003). We thank all the staff in Far Eastern Hydrometeorology and Environmental Monitoring (Roshydromet). All Amur River dFe concentration and discharge data were provided by Roshydromet under project C-04 of the Research Institute for Humanity and Nature (RIHN), Japan, entitled "Human Activities in Northeastern Asia and Their Impact on the Biological Productivity in North Pacific Ocean", with Takayuki Shiraiwa as the principal investigator between 2005 and 2009. We thank Tina Tin, PhD, from Edanz (https://jp.edanz.com/ac) for editing a draft of this manuscript.

Author contributions
YT conceived the study and analysed the data with significant input from TH, HK, and MK. YT wrote the paper with substantial help from TH and HK with regard to data handling and interpretation of results. All authors discussed the results of the study, reviewed the final manuscript, and approved the manuscript submission.

Funding
This research was funded by the Japan Society for the Promotion of Science (JSPS) KAKENHI (Grant Number 19H05668) project entitled "Pan-Arctic Water-Carbon Cycles (PAWCs)" (https://enpawcs.home.blog/). It was also supported by the Japan Science and Technology Agency (JST) Belmont Forum (Grant Number JPMJBF2003).

Availability of data and materials
Data of dFe concentration in the Amur River are available in the Figshare repository, https://doi.org/https://doi.org/10.6084/m9.figshare.20550891. Climatic Research Unit gridded Time Series v4.05 (CRU) data are available at: https://www.uea.ac.uk/groups-and-centres/climatic-research-unit. Japanese Reanalysis Project (JRA-55, 1.25°×1.25°) data are available at: https://jra.kishou.go.jp/JRA-55/index_ja.html. PDO index data from Japan Meteorological Agency are available at: https://www.data.jma.go.jp/gmd/kaiyou/data/shindan/b_1/pdo/pdo.html

Declarations

Competing interests
The authors declare that they have no competing interest.

Author details
[1]Institute for Space–Earth Environmental Research, Nagoya University, Nagoya, Aichi 464-8601, Japan. [2]The IDEC Institute - Center for Peaceful and Sustainable Futures (CEPEAS), Network for Education and Research On Peace and Sustainability (NERPS), Graduate School of Humanities and Social Sciences International Economic Development Program (IEDP), Graduate School of Innovation and Practice for Smart Society (SmaSo), Seto Inland Sea Carbon Neutral Research Center, Hiroshima University, Higashi-Hiroshima, Hiroshima 739-8529, Japan.

Received: 28 August 2023 Accepted: 15 March 2024
Published online: 26 March 2024

References

Abesser C, Robinson R, Soulsby C (2006) Iron and manganese cycling in the storm runoff of a Scottish upland catchment. J Hydrol 326:59–78. https://doi.org/10.1016/j.jhydrol.2005.10.034

Aiken GR, Spencer RGM, Striegl RG, Schuster PF, Raymond PA (2014) Influences of glacier melt and permafrost thaw on the age of dissolved organic carbon in the Yukon River basin. Glob Biogeochem Cycles 28:525–537. https://doi.org/10.1002/2013GB004764

Andersson K, Dahlqvist R, Turner D, Stolpe B, Larsson T, Ingri J, Andersson P (2006) Colloidal rare earth elements in a boreal river: Changing sources and distributions during the spring flood. Geochim Cosmochim Acta 70:3261–3274. https://doi.org/10.1016/j.gca.2006.04.021

Bagard ML, Chabaux F, Pokrovsky OS, Viers J, Prokushkin AS, Pa S, Rihs S, Schmitt A, Dupre B (2011) Seasonal variability of element fluxes in two Central Siberian rivers draining high latitude permafrost dominated areas. Geochim Cosmochim Acta 75:3335–3357. https://doi.org/10.1016/j.gca.2011.03.024

Bruland KW, Lohan MC (2003) Controls of Trace Metals in Seawater. In: Heinrich DH, Karl KT (eds) Treatise on Geochemistry. Elsevier, Amsterdam, pp 23–47

Colombo N, Salerno F, Gruber S, Freppaz M, Williams M, Fratianni S, Giardino M (2018) Review: impacts of permafrost degradation on inorganic chemistry of surface fresh water. Glob Planet Change 162:69–83. https://doi.org/10.1016/j.gloplacha.2017.11.017

Connon RF, Quinton WL, Craig JR, Hayashi M (2014) Changing hydrologic connectivity due to permafrost thaw in the lower Liard River valley, NWT. Canada Hydrol Process 28:4163–4178. https://doi.org/10.1002/hyp.10206

Douglas TA, Turetsky MR, Koven CD (2020) Increased rainfall stimulates permafrost thaw across a variety of Interior Alaskan boreal ecosystems. NPJ Clim Atmos Sci 3:1–7. https://doi.org/10.1038/s41612-020-0130-4

Drake TW, Guillemette F, Hemingway JD, Podgorski DC, Zimov NS, Spencer RGM (2018) Increasing alkalinity export from large Russian Arctic rivers. Environ Sci Technol 52:8302–8308. https://doi.org/10.1021/acs.est.8b01051

Evans SG, Yokeley B, Stephens C, Brewer B (2020) Potential mechanistic causes of increased baseflow across northern Eurasia catchments underlain by permafrost. Hydrol Process 34:2676–2690. https://doi.org/10.1002/hyp.13759

Frey KE, McClelland JW (2009) Impacts of permafrost degradation on arctic river biogeochemistry. Hydrol Process 23:169–182. https://doi.org/10.1002/hyp.7196

Frey KE, McClelland JW, Holmes RM, Smith LG (2007) Impacts of climate warming and permafrost thaw on the riverine transport of nitrogen and phosphorus to the Kara Sea. JGR Biogeosci 112:1–10. https://doi.org/10.1029/2006JG000369

Ganzey SS, Ermoshin VV, Mishina NV, (2010) the landscape changes after 1930 using two kinds of land use maps (1930 and 2000). In: Shiraiwa (ed) Report on Amur-Okhotsk Project, vol 6. Research Institute for Humanity and Nature, Kyoto, pp 251–262. http://id.nii.ac.jp/1422/00002691/

Harris I, Osborn TJ, Jones P, Lister D (2020) Version 4 of the CRU TS monthly high-resolution gridded multivariate climate dataset. Sci Data 7:1–18. https://doi.org/10.1038/s41597-020-0453-3

Herndon EM, Yang Z, Bargar J, Janot N, Regier TZ, Graham DE, Wullschleger SD, Gu B, Liang L (2015) Geochemical drivers of organic matter decomposition in arctic tundra soils. Biogeochemistry 126:397–414. https://doi.org/10.1007/s10533-015-0165-5

Hinkel KM, Paetzold F, Nelson FE, Bockheim JG (2001) Patterns of soil temperature and moisture in the active layer and upper permafrost at Barrow, Alaska: 1993–1999. Glob Planet Change 29:293–309. https://doi.org/10.1016/S0921-8181(01)00096-0

Holmes RM, McClelland JW, Peterson BJ, Tank SE, Bulygina E, Eglinton TI, Gordeev VV, Gurtovaya TY, Raymond PA, Repeta DJ, Staples R, Striegl RG, Zhulidov AV, Zimov SA (2012) Seasonal and annual fluxes of nutrients and organic matter from large rivers to the arctic ocean and surrounding seas. Estuaries Coast 35:369–382. https://doi.org/10.1007/s12237-011-9386-6

Hydrochemical Institute (2006) Russian international technical standards 52.24.358–2006: Mass concentration of total Fe in waters. https://files.stroyinf.ru/Index2/1/4293837/4293837319.htm [In Russian]

Ilina SM, Poitrasson F, Lapitskiy SA, Alekhin YV (2013) Extreme iron isotope fractionation between colloids and particles of boreal and temperate organic-rich waters. Geochim Cosmochim Acta 101:96–111. https://doi.org/10.1016/j.gca.2012.10.023

Ingri J, Conrad S, Lidman F, Nordblad F, Engström E, Rodushkin I, Porcelli D (2018) Iron isotope pathways in the boreal landscape: Role of the riparian zone. Geochim Cosmochim Acta 239:49–60. https://doi.org/10.1016/j.gca.2018.07.030

Jessen S, Holmslykke HD, Rasmussen K, Richardt N, Holm PE (2014) Hydrology and pore water chemistry in a permafrost wetland, Ilulissat, Greenland. Water Resour Res 50:4760–4774. https://doi.org/10.1002/2013WR014376

Kawahigashi M, Kaiser K, Kalbitz K, Rodionov A, Guggenberger G (2004) Dissolved organic matter in small streams along a gradient from discontinuous to continuous permafrost. Glob Change Biol 10:1576–1586. https://doi.org/10.1111/j.1365-2486.2004.00827.x

Kobayashi S, Ota Y, Harada Y, Ebita A, Moriya M, Onoda H, Onogi K, Kamahori H, Kobayashi C, Endo H, Miyaoka K, Takahashi K (2015) The JRA-55 reanalysis: General specifications and basic characteristics. J Meteor Soc Japan 93:5–48. https://doi.org/10.2151/jmsj.2015-001

Kokeji SV, Burn CR (2005) Geochemistry of the active layer and near-surface permafrost, Mackenzie delta region, Northwest Territories, Canada. Can J Earth Sci 42:37–48. https://doi.org/10.1139/E04-089

Kolosov RR, Prokushkin AS, Pokrovsky OS (2016) Major anion and cation fluxes from the Central SiberianPlateau watersheds with underlying permafrost. IOP Conf Ser Earth Environ Sci 48:012018. https://doi.org/10.1088/1755-1315/48/1/012018

Kritzberg ES, Ekström SM (2012) Increasing iron concentrations in surface waters–A factor behind brownification? Biogeosciences 9:1465–1478. https://doi.org/10.5194/bg-9-1465-2012

Laglera LM, Van Den Berg CMG (2009) Evidence for geochemical control of iron by humic substances in seawater. Limnol Oceanogr 54:610–619. https://doi.org/10.4319/lo.2009.54.2.0610

Levshina SI (2012) Iron distribution in surface waters in the Middle and Lower Amur basin. Water Resour 39:375–383. https://doi.org/10.1134/s0097807812040082

Levshina SI (2016) Geochemistry of organic matter in river waters of the Amur basin, Russia. Environ Earth Sci 75:1–10. https://doi.org/10.1007/s12665-015-5202-0

Lipson DA, Zona D, Raab TK, Bozzolo F, Mauritz M, Oechel WC (2012) Water-table height and microtopography control biogeochemical cycling in an Arctic coastal tundra ecosystem. Biogeosciences 9:577–591. https://doi.org/10.5194/bg-9-577-2012

Liu Y, Sun C, Hao Z, He B (2022) Periodic decadal swings in dry/wet conditions over Central Asia. Environ Res Lett 17:054050. https://doi.org/10.1088/1748-9326/ac6c3b

Mantua NJ, Hare SR, Zhang Y, Wallace JM, Francis RC (1997) A pacific interdecadal climate oscillation with impacts on salmon production; Bull. Amer Meteor Soc 78:1069–1079. https://doi.org/10.1175/1520-0477(1997)078%3c1069:APICOW%3e2.0.CO;2

Martin JH, Fitzwater SE (1988) Iron deficiency limits phytoplankton growth in the north-east Pacific subarctic. Nature 331:341–343. https://doi.org/10.1038/331341a0

Martin JH, Gordon RM, Fitzwater SE, Broenkow WW (1989) Vertex: phytoplankton/iron studies in the Gulf of Alaska. Deep-Sea Res I: Oceanogr Res Pap 36:649–680. https://doi.org/10.1016/0198-0149(89)90144-1

Martin JH, Gordon RM, Fitzwater SE (1990) Iron in Antarctic waters. Nature 345:156–158. https://doi.org/10.1038/345156a0

Martin JH, Coale KH, Johnson KS, Fitzwater SE, Gordon RM, Tanner SJ, Hunter CN, Elrod VA, Nowicki JL, Coley TL, Barber RT, Lindley S, Watson AJ, Van Scoy K, Law CS, Liddicoat MI, Ling R, Stanton T, Stockel J, Collins C, Anderson A, Bidigare R, Ondrusek M, Latasa M, Millero FJ, Lee K, Yao W, Zhang JZ, Friederich G, Sakamoto C, Chavez F, Buck K, Kolber Z, Greene R, Falkowski P, Chisholm SW, Hoge F, Swift R, Yungel J, Turner S, Nightingale P, Hatton A, Liss P, Tindale NW (1994) Testing the iron hypothesis in ecosystems of the equatorial Pacific Ocean. Nature 371:123–129. https://doi.org/10.1038/371123a0

Matsunaga K, Nishioka J, Kuma K, Toya K, Suzuki Y (1998) Riverine input of bioavailable iron supporting phytoplankton growth in Kesennuma Bay (Japan). Water Res 32:3436–3442. https://doi.org/10.1016/S0043-1354(98)00113-4

McClelland JW, Stieglitz M, Pan F, Holmes RM, Peterson BJ (2007) Recent changes in nitrate and dissolved organic carbon export from the upper Kuparuk River, North Slope. Alaska JGR: Biogeosciences 112:1–13. https://doi.org/10.1029/2006JG000371

Mokhov II, Semenov VA (2016) Weather and climate anomalies in russian regions related to global climate change. Russ Meteorol Hydrol 41:84–92. https://doi.org/10.3103/S1068373916020023

Moore JK, Braucher O (2008) Sedimentary and mineral dust sources of dissolved iron to the world ocean. Biogeosciences 5:631–656. https://doi.org/10.5194/bg-5-631-2008

Nagao, S. Terashima M, Kodama H, Kim VI, Shesterkin PV, Makhinov AN, (2007) Migration behavior of Fe in the Amur River Basin. In: Shiraiwa (ed) Report on Amur-Okhotsk Project, vol 4. Research Institute for Humanity and Nature, Kyoto, pp 37–48. http://id.nii.ac.jp/1422/00002607/

Nishioka J, Nakatsuka T, Watanabe YW, Yasuda I, Kuma K, Ogawa H, Ebuchi N, Scherbinin A, Volkov YN, Shiraiwa T, Wakatsuchi M (2013) Intensive mixing along an island chain controls oceanic biogeochemical cycles. Glob Biogeochem Cycles 27:920–929. https://doi.org/10.1002/gbc.20088

Nishioka J, Nakatsuka T, Ono K, Volkov YN, Scherbinin A, Shiraiwa T (2014) Quantitative evaluation of iron transport processes in the Sea of Okhotsk. Prog Oceanogr 126:180–193. https://doi.org/10.1016/j.pocean.2014.04.011

Novorotskii PV (2007) Climate changes in the Amur River basin in the last 115 years. Russ Meteorol Hydrol 32:102–109. https://doi.org/10.3103/S1068373907020045

Olefeldt D, Persson A, Turetsky MR (2014) Influence of the permafrost boundary on dissolved organic matter characteristics in rivers within the Boreal and Taiga plains of western Canada. Environ Res Lett 9:035005. https://doi.org/10.1088/1748-9326/9/3/035005

Onishi T, Yoh M, Yan B, Kawahigashi M, (2009) Evaluation of agricultural activity impacts on dissolved iron flux in the Sanjiang Plain, China. In: Abstracts of the Japanese society of irrigation, drainage and rural engineering proceedings conference, University of Tsukuba, Ibaraki, 4–6 August 2009. [In Japanese]

Palviainen M, Lehtoranta J, Ekholm P, Ruoho-Airola T, Kortelainen P (2015) Land cover controls the export of terminal electron acceptors from boreal catchments. Ecosystems 18:343–358. https://doi.org/10.1007/s10021-014-9832-y

Pan XF, Yan BX, Yoh M (2011) Effects of land use and changes in cover on the transformation and transportation of iron: a case study of the Sanjiang Plain, Northeast China. Sci China Earth Sci 54:686–693. https://doi.org/10.1007/s11430-010-4082-0

Peixoto JP, Oort AH, (1983) The atmospheric branch of the hydrological cycle and climate: In Street-Perrott A, Beran M, Ratcliffe R (eds) Variations in the Global Water Budget, Springer, Dordrecht, pp 5–65. https://doi.org/10.1007/978-94-009-6954-4_2

Peixoto JP, Oort AH (1992) Physics of Climate. American Institute of Physics, New York

Petrone KC, Jones JB, Hinzman LD, Boone RD (2006) Seasonal export of carbon, nitrogen, and major solutes from Alaskan catchments with discontinuous permafrost. JGR Biogeosciences 111:1–13. https://doi.org/10.1029/2005JG000055

Pokrovsky OS, Manasypov RM, Loiko SV, Shirokova LS, Krickov IA, Pokrovsky BG, Kolesnichenko LG, Kopysov SG, Zemtzov VA, Kulizhsky SP, Vorobyev SN, Kirpotin SN (2015) Permafrost coverage, watershed area and season control of dissolved carbon and major elements in western Siberian rivers. Biogeosciences 12:6301–6320. https://doi.org/10.5194/bg-12-6301-2015

Pokrovsky OS, Manasypov RM, Loiko SV, Krickov IA, Kopysov SG, Kolesnichenko LG, Vorobyev SN, Kirpotin SN (2016) Trace element transport in western Siberian rivers across a permafrost gradient. Biogeosciences 13:1877–1900. https://doi.org/10.5194/bg-13-1877-2016

Price NM, Ahner BA, Morel FMM (1994) The equatorial Pacific Ocean: grazer-controlled phytoplankton populations in an iron-limited ecosystem. Limnol Oceanogr 39:520–534. https://doi.org/10.4319/lo.1994.39.3.0520

Quinton WL, Hayashi M, Carey SK (2008) Peat hydraulic conductivity in cold regions and its relation to pore size and geometry. Hydrol Process 22:2829–2837. https://doi.org/10.1002/hyp

Quinton WL, Hayashi M, Chasmer LE (2009) Peatland hydrology of discontinuous permafrost in the northwest territories: overview and synthesis. Can Water Resour J 34:311–328. https://doi.org/10.4296/cwrj3404311

Rember RD, Trefry JH (2004) Increased concentrations of dissolved trace metals and organic carbon during snowmelt in rivers of the alaskan arctic. Geochim Cosmochim Acta 68:477–489. https://doi.org/10.1016/S0016-7037(03)00458-7

Sarkkola S, Nieminen M, Koivusalo H, Laurén A, Kortelainen P, Mattsson T, Palviainen M, Piirainen S, Starr M, Finér L (2013) Iron concentrations are increasing in surface waters from forested headwater catchments in eastern Finland. Sci Total Environ 463–464:683–689. https://doi.org/10.1016/j.scitotenv.2013.06.072

Shamov VV, Onishi T, Kulakov VV (2014) Dissolved Iron Runoff in Amur Basin Rivers in the Late XX Century. Water Res 41:201–209. https://doi.org/10.1134/S0097807814020122

Shesterkin VP, Talovskaya HM, Shesterkina HM (2013) Long-standing dynamics of iron content and flow in the water of the middle Amur River during the lowest winter water level. Russ J Pacific Geol 32:106–111 (**In Russian**)

Shiraiwa T (2012) "Giant Fish-Breeding Forest": A New Environmental System Linking Continental Watershed with Open Water. In: Taniguchi M, Shiraiwa T (eds) The Dilemma of Boundaries. Springer, Tokyo, pp 73–85. https://doi.org/10.1007/978-4-431-54035-9_8

Sokolova GV, Verkhoturov AL, Korolev SP (2019) Impact of deforestation on streamflow in the amur river basin. Geosciences 9:262. https://doi.org/10.3390/geosciences9060262

Sorokin YI, Sorokin PY (1999) Production in the sea of Okhotsk. J Plankton Res 21:201–230. https://doi.org/10.1093/plankt/21.2.201

Striegl RG, Aiken GR, Dornblaser MM, Raymond PA, Wickland KP (2005) A decrease in discharge-normalized DOC export by the Yukon River during summer through autumn. Geophys Res Lett 32:1–4. https://doi.org/10.1029/2005GL024413

Sunda WG (2012) Feedback interactions between trace metal nutrients and phytoplankton in the ocean. Front Microbiol 3:1–22. https://doi.org/10.3389/fmicb.2012.00204

Suzuki K, Hattori-Saito A, Sekiguchi Y, Nishioka J, Shigemitsu M, Isada T, Liu H, McKay RML (2014) Spatial variability in iron nutritional status of large diatoms in the Sea of Okhotsk with special reference to the Amur River discharge. Biogeosciences 11:2503–2517. https://doi.org/10.5194/bg-11-2503-2014

Takeda S, Obata H (1995) Response of equatorial Pacific phytoplankton to subnanomolar Fe enrichment. Mar Chem 50:219–227. https://doi.org/10.1016/0304-4203(95)00037-R

Tank SE, Striegl RG, McClelland JW, Kokelj SV (2016) Multi-decadal increases in dissolved organic carbon and alkalinity flux from the Mackenzie drainage basin to the Arctic Ocean. Environ Res Lett 11:054015. https://doi.org/10.1088/1748-9326/11/5/054015

Tashiro Y, Yoh M, Shiraiwa T, Onishi T, Shesterkin V, Kim V (2020) Seasonal variations of dissolved iron concentration in active layer and rivers in permafrost areas. Russian Far East Water 12:2579. https://doi.org/10.3390/w12092579

Tashiro Y, Yoh M, Shesterkin VP, Shiraiwa T, Onishi T, Naito D (2023) Permafrost Wetlands Are Sources of Dissolved Iron and Dissolved Organic Carbon to the Amur-Mid Rivers in Summer. J Geophys Res Biogeosci 128:e2023JG007481. https://doi.org/10.1029/2023JG007481

Toohey RC, Herman-Mercer NM, Schuster PF, Mutter EA, Koch JC (2016) Multi-decadal increases in the Yukon River Basin of chemical fluxes as indicators of changing flowpaths, groundwater, and permafrost. Geophys Res Lett 43:120–130. https://doi.org/10.1002/2016GL070817

Vorobyev SN, Pokrovsky OS, Serikova S, Manasypov RM, Krickov IV, Shirokova LS, Lim A, Kolesnichenko LG, Kirpotin SN, Karlsson J (2017) Permafrost boundary shift in Western Siberia may not modify dissolved nutrient concentrations in rivers. Water 9:985. https://doi.org/10.3390/w9120985

Vorobyev SN, Pokrovsky OS, Kolesnichenko LG, Manasypov RM, Shirokova LS, Karlsson J, Kirpotin SN (2019) Biogeochemistry of dissolved carbon, major, and trace elements during spring flood periods on the Ob River. Hydrol Process 33:1579–1594. https://doi.org/10.1002/hyp.13424

Wang L, Yan B, Pan X, Zhu H (2012) The spatial variation and factors controlling the concentration of total dissolved iron in rivers, Sanjiang Plain. Clean - Soil Air Water 40:712–717. https://doi.org/10.1002/clen.201100251

Yan B, Guan J, Shesterkin V, Zhu H (2016) Variations of dissolved iron in the Amur River during an extreme flood event in 2013. Chin Geogr Sci 26(5):679–686. https://doi.org/10.1007/s11769-016-0828-8

Zhang G, Zeng G, Li C, Yang X (2020) Impact of PDO and AMO on interdecadal variability in extreme high temperatures in North China over the most recent 40-year period. Clim Dyn 54:3003–3020. https://doi.org/10.1007/s00382-020-05155-z

Publisher's Note

Yuto Tashiro received a Ph.D. in Agricultural Science from Tokyo University of Agriculture and Technology in 2021. YT is a postdoctoral researcher at the Institute for Space-Earth Environmental Research, Nagoya University.

Tetsuya Hiyama received a Ph.D. in science from the University of Tsukuba in 1995. TH is the principal investigator of the JSPS Grantin-Aid for Scientific Research (KAKENHI) project entitled "Pan-Arctic Water-Carbon Cycles (PAWCs)".

Hironari Kanamori received a Ph.D. in science from Graduate School of Environmental Studies, Nagoya University in 2015. HK is a researcher at the Institute for Space-Earth Environmental Research, Nagoya University.

Masayuki Kondo received a Ph.D. in Agricultural Science from Hokkaido University in 2015. MK is the director of the sustainability division of the Seto Inland Sea Carbon Neutral Research Center (S-CNC) in Hiroshima University.